Biochemical and Biophysical Research Communications 447 (2014) 26–31

Contents lists available at ScienceDirect

Biochemical and Biophysical Research Communications

journal homepage: www.elsevier.com/locate/ybbrc

Basic Tilted Helix Bundle – A new protein fold in human FKBP25/FKBP3 and HectD1

Sara Helander [a,1], Meri Montecchio [a,1], Alexander Lemak [b,c], Christophe Farès [b,2], Jonas Almlöf [a,3], Yanjun Li [d], Adelinda Yee [b,c], Cheryl H. Arrowsmith [b,c,d], Sirano Dhe-Paganon [d,4], Maria Sunnerhagen [a,*]

[a] Department of Physics, Chemistry and Biology, Division of Chemistry, Linköping University, SE-58183 Linköping, Sweden
[b] Princess Margaret Cancer Centre and Department of Medical Biophysics, University of Toronto, Toronto, Ontario M5G 1L7, Canada
[c] Northeast Structural Genomics Consortium, Toronto, Ontario, Canada
[d] Structural Genomics Consortium, University of Toronto, 101 College St, Toronto, Ontario M5G 1L7, Canada

ARTICLE INFO

Article history:
Received 11 March 2014
Available online 22 March 2014

Keywords:
Immunophillins
NMR structure
Structural genomics
FKBP25
FKBP3
HectD1
YY1

ABSTRACT

In this paper, we describe the structure of a N-terminal domain motif in nuclear-localized FKBP25$_{1-73}$, a member of the FKBP family, together with the structure of a sequence-related subdomain of the E3 ubiquitin ligase HectD1 that we show belongs to the same fold. This motif adopts a compact 5-helix bundle which we name the Basic Tilted Helix Bundle (BTHB) domain. A positively charged surface patch, structurally centered around the tilted helix H4, is present in both FKBP25 and HectD1 and is conserved in both proteins, suggesting a conserved functional role. We provide detailed comparative analysis of the structures of the two proteins and their sequence similarities, and analysis of the interaction of the proposed FKBP25 binding protein YY1. We suggest that the basic motif in BTHB is involved in the observed DNA binding of FKBP25, and that the function of this domain can be affected by regulatory YY1 binding and/or interactions with adjacent domains.

© 2014 Elsevier Inc. All rights reserved.

1. Introduction

FK506-binding proteins (FKBPs) belong to the family of the immunophilins first defined by their joint property of binding immunosuppressant drugs such as FK506 and rapamycin [1]. The conserved immunosuppressant binding site is located in the common peptidylprolyl cis–trans isomerase (PPIase) domain, where drug binding hampers further interactions with proteins such as calcineurin and mTOR leading to decreased T-cell proliferation [1,2]. The PPIase domain in FKBPs can occur singly or in multiple copies, and is flanked by various other modules and/or sequence motifs depending on function and cellular localization [2]. The first of the immunophilins discovered in the nucleus was FKBP3 [3], now predominantly known as FKBP25, which is the name we will use throughout [2,4].

FKBP25 is a small protein (25 kDa) FKBP with two domains: a C-terminal PPIase domain, and an N-terminal basic domain found only in mammalian orthologs. Whereas the structure of its C-terminal PPIase domain was solved in complex with rapamycin [5] (PDB id 1PBK), the N-terminal domain, with hitherto unknown structure, was found to bind both nucleolin/C23 [6] and DNA [7]. By analogy with FKBPs in plants and yeast which contain nucleolin-like domains and thereby may have similar functions as nucleolin in chromatin remodeling [8], the N-terminal domain of FKBP25 has been suggested to have a role in regulating the association state of nucleosomes by interacting with nucleolin [4]. Moreover, this basic domain in FKBP25 forms alternative complexes with other chromatin-related proteins, such as the HDAC1, HDAC2, and the transcriptional regulator YY1, the DNA binding activity of which is enhanced on binding FKBP25 [9].

Human HectD1 is a 2612-residue HECT superfamily E3 ubiquitin ligase containing 4 recognizable domains: ANK repeats, a SAD domain, a MIB/HERC2 domain, and a HECT E3 ligase domain. HectD1 knockout mice show perinatal lethality, exencephaly, impaired neural fold elevation, abnormal head mesenchyme morphology, and defects in eye and cranial vault morphology [10]. Cell studies suggest that the Adenomatous Polyposis Coli (APC) protein is modified at Lys-63 by HectD1 with polyubiquitin to promote APC-Axin interaction, and thereby affecting cell fate and cell

* Corresponding author. Fax: +46 13 13 75 68.
E-mail address: maria.sunnerhagen@liu.se (M. Sunnerhagen).
[1] These authors contributed equally.
[2] Current address: Max-Planck-Institut für Kohlenforschung, Kaiser-Wilhelm-Platz 1, 45470 Mülheim and der Ruhr, Germany.
[3] Current address: Department of Medical Sciences, Molecular Medicine and Science for Life Laboratory, Uppsala University, Uppsala 75123, Sweden.
[4] Current address: Department of Cancer Biology, Dana–Farber Cancer Institute, Boston, MA 02215, USA.

http://dx.doi.org/10.1016/j.bbrc.2014.03.068
0006-291X/© 2014 Elsevier Inc. All rights reserved.

homeostasis [11]. Moreover, HectD1 regulates intracellular localization and secretion of Hsp90 to promote correct neural tube closure in mice [10].

During our structural genomic efforts, we discovered an additional domain within HectD1, between residues 1879–1966. Interestingly, we found that the fold of this domain is similar to that of the N-terminal domain of FKBP25. Here we present these two structures: the N-terminal domain $FKBP25_{1-73}$, and the sequence-wise distant but structure-wise similar domain of $HectD1_{1879-1966}$. Although the function of these domains remains unknown, by comparing the two structures and their sequence conservation, and by performing the additional ligand titration with the proposed FKBP25 binding protein YY1, we put forward a hypothesis on the location of interaction surfaces that are shared and not shared between FKBP25 and HectD1.

2. Methods

2.1. Cloning, expression, and purification

The N-terminal residues 1–73 of FK506 binding protein 3, 25 kDa (FKBP3, also known as FKBP-25; PPIase) was cloned from a Mammalian Gene Collection cDNA template (fkbp03.BC020809.MGC.AU84-G12.pDNR-LIB) and region 1881–1968 of HECT domain containing 1 (HectD1) was cloned from a Kazusa cDNA template (hectd1.BAA86445.KZA.KIAA1131.pBluescriptSK+) into the pET28a-LIC (GenBank, EF442785) and pET28MHL (GenBank, EF456735) vector, respectively using the In-Fusion CF Dry-Down PCR Cloning Kit (Clontech, 639605).

A 250-ml flask containing M9 base minimum media (with ^{13}C-glucose and ^{15}N $(NH_4)_2SO_4$) supplemented with 50 μg/ml kanamycin (BioShop Canada KAN 201) was inoculated from a fresh transformed plate of BL-21(DE3) CodonPlus. The flask was shaken overnight (16 h) at 250 rpm at 37 °C. Using the Lex system, a 2-L bottle (VWR 89000-242) containing 1800 ml of minimum media supplemented 50 μg/ml kanamycin and 600 μl antifoam 204 (Sigma A-8311) was inoculated with 50 ml overnight LB culture, and incubated at 37 °C. The temperature of the media was reduced to 15 °C one hour prior to induction and induced at $OD_{(600)} = 2$ with 100 μM isopropyl-thio-β-D-galactopyranoside (BioShop Canada IPT 001). Cultures were aerated overnight (16 h) at 15 °C, and cell pellets collected by centrifugation and frozen at −80 °C.

Frozen cell pellet contained in bags (Beckman 369256) obtained from 2 L of culture were thawed by soaking in warm water. Each cell pellet was resuspended in 25–40 ml lysis buffer and homogenized using an Ultra-Turrax T8 homogenizer (IKA Works) at maximal setting for 30–60 s per pellet. Cell lysis was accomplished by sonication (Virtis408912, Virsonic) on ice: the sonication protocol was 10-s pulse at half-maximal frequency (5.0), 10-s rest, for 10-min total sonication time per pellet. Unclarified lysate was mixed with 2–3 ml of Ni-NTA superflow Resin (Qiagen) per 40 ml lysate. The mixture was incubated with mixing for at least 45 min at 4 °C. The mixture was than loaded onto an empty column (BioRad) and washed with 100 ml wash buffer. Samples were eluted from the resin by exposure to 2–3 column volumes (approx. 10–15 ml) of elution buffer. An XK 26 × 65 column (GE Healthcare) packed with HighLoad Superdex 75 resin (GE Healthcare) was pre-equilibrated with gel filtration buffer for 1.5 column volumes using an AKTA explorer (GE Healthcare) at a flow rate of 2.5 ml/min. The eluate sample from the IMAC step (approx. 15 ml) was loaded onto the column at 1.5 ml/min, and 2-ml fractions were collected into 96-well plates (VWR 40002-012) using peak fractionation protocols). Fractions observed by a UV absorption chromatogram to contain the protein were pooled. Purified proteins were concentrated using 15-ml concentrators with a 5000 molecular weight cut-off (Amicon Ultra-15, UFC900524, Millipore) at 3750 rpm, typically resulting in a final concentration of 4–5 mg/ml. Lysis buffer: 1× PBS, 250 mM NaCl, 5 mM imidazole, 1 mM phenylmethanesulfonyl fluoride, and 100 μl Sigma general protease inhibitor (Sigma P2714-1BTL, resuspended according to manufacturer's instructions); Wash buffer: 1× PBS, 250 mM NaCl, 20 mM imidazole; Elution buffer: 1× PBS, 250 mM NaCl, 250 mM imidazole; Gel filtration buffer: 1× PBS, 250 mM NaCl, 2 mM DTT.

The pET28-MHL vector containing the gene for the His-tagged $YY1_{293-350}$, comprises the proposed FKBP25 interaction site $YY1_{300-333}$ [9] as well as an extended C-terminus to including two complete zinc fingers [12] (PDB id 1UBD). *Escherichia coli* BL21(DE3) pLysS cells were transformed using electroporation, cultured at 37 °C in 2 L of LB-Kan-Cam and induced with 1 mM IPTG at $OD_{600} = 1.0$, jointly with adding10 μM $ZnCl_2$. The cells were incubated at 22 °C overnight, harvested by centrifugation at 4 °C, and the pellet resuspended in lysis buffer at pH 8.0 (50 mM NaH_2PO_4, 300 mM NaCl, 10 mM imidazole, 10 mM β-merchaptoethanol; with complete protease inhibitor (Roche)), lysed by sonication and centrifuged at 13000*g*, 4 °C, 30 min. The YY1 protein was purified from the supernatant using cobalt-charged TALON metal affinity resin (Clonetech) washed prior to and after sample loading with 15 column volumes of lysis buffer. Elution was performed stepwise in lysis buffer, pH 8.0, with 20–250 mM imidazole. Fractions containing $YY1_{293-350}$ as judged from SDS–PAGE were dialysed against gel filtration buffer (10 mM Tris, 300 mM NaCl, 10 mM DTT, pH 7.0) and separated from residual impurities on a HiLoad 16/60 Superdex 75 gel filtration column (GE Healthcare).

2.2. NMR spectroscopy

NMR spectra were recorded at 25 °C on Varian Inova 600, Bruker Avance 600 MHz or 800 MHz spectrometers equipped with a cryogenically cooled probehead. Both structures were determined in a streamlined, integrated strategy using a limited set of non-uniformly sampled 3D NMR spectra, ABACUS, and CYANA [13]. For both proteins, HNCO, CBCA(CO)NH, HBHA(CO)NH, HNCA, (H)CCH-TOCSY and H(C)CH-TOCSY, ^{15}N-edited NOESY-HSQC (t_m = 100 ms), and ^{13}C-edited aliphatic and aromatic NOESY-HSQC and TOCSY-HSQC in H_2O (t_m = 100 ms) spectra were employed, where peak picking was performed manually using Sparky [14]. NOESY peaks were assigned in iterative cycles of automated structure calculation and NOE assignment USING CYANA 2.0 [15]. For FKBP25, anisotropic media for measurement of dipolar couplings was prepared by addition of filamentous phages (Pf1) (ASLA Biotech, Riga) to a concentration of 5 mg/ml. The ^1J and $^1J + ^1D$ splittings were measured under isotropic and anisotropic conditions, respectively, on an Avance 600 Bruker instrument equipped with a cryogenically-cooled probehead with the experiments 2D IPAP-^{1}H-^{15}N HSQC (for $^1J(+^1D)_{HNN}$) [16], 3D HNCO-IPAP (for $^1J(+^1D)_{CC\alpha'}$ and $^1J(+^1D)_{HNC\alpha}$) and 3D HNCO-IPAP (for $^1J(+^1D)_{NC'}$) [17] using time-optimized strategies, when advantageous, such as Band-selective Excitation Short-Transient (BEST) for rapid repetition [18] or non-uniform sampling (NUS) with multidimension decomposition (MDD) for sparse acquisition [19]. A total of 293 RDCs (68HN, 56 CaCo, 56HCa and 63 NCo) were extracted of which 138 were retained for final structure refinement based on error estimation and secondary structure elements. The RDCs fit to the structure was analysed using PALES [20]. The final 20 lowest-energy structures were refined with the CNS [21] package by performing a short constrained molecular dynamics simulation in explicit solvent [22]. The resulting structures were analyzed using the PSVS validation software [23]. The final refined ensembles of 20 structures and resonance assignments for $FKBP25_{1-73}$ and $HectD1_{1879-1966}$ were deposited into the Protein Data Bank and BioMagRes DB with accession codes 2KFV, 16189 and 2LC3,

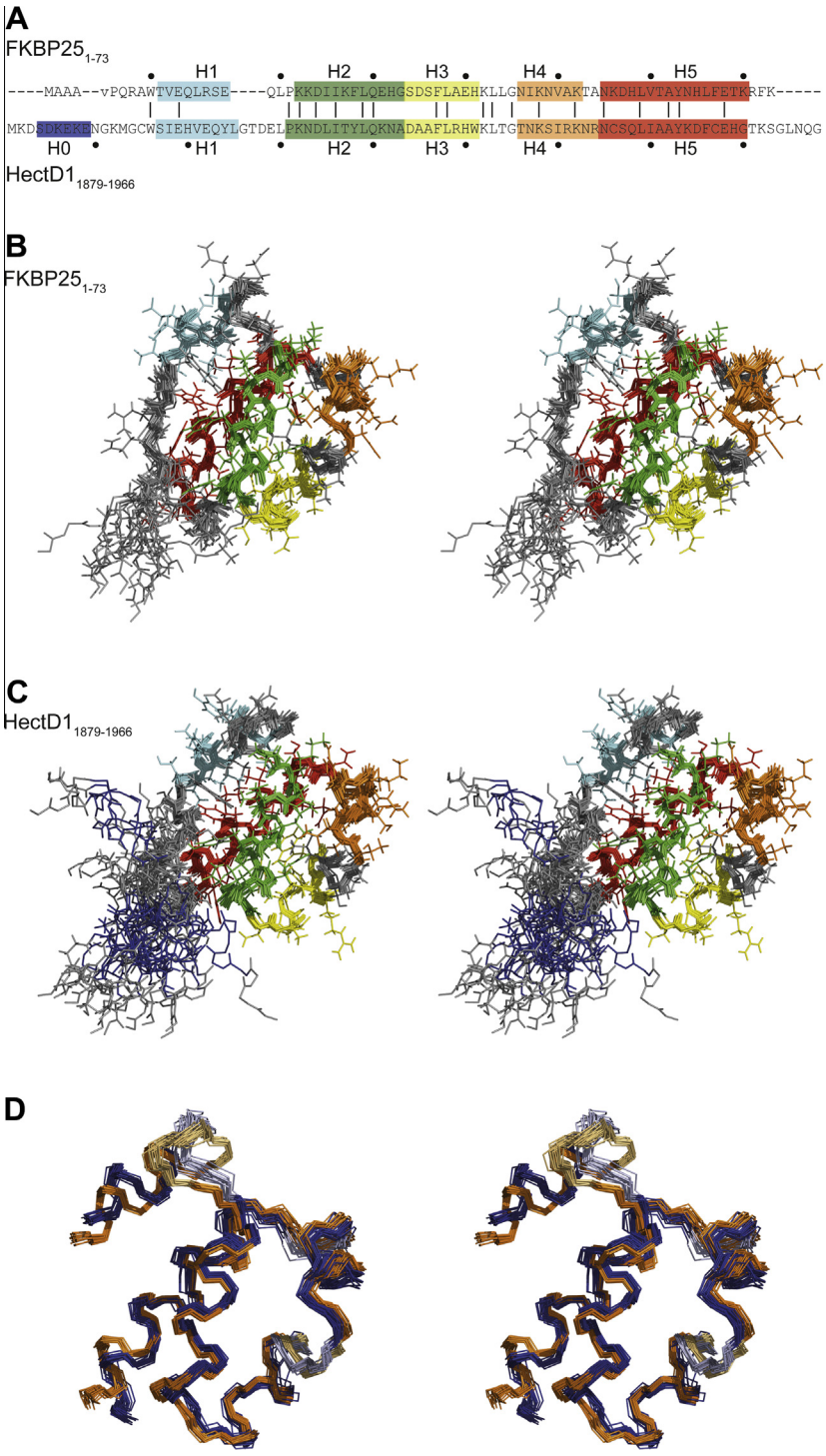

Fig. 1. Sequence alignment (A) between $FKBP25_{1-73}$ and $HectD1_{1879-1966}$, with every tenth amino acid in each sequence marked by a dot. Structurally non-equivalent residues (e.g., in loops) are in lowercase. Stereo view of $FKBP25_{1-73}$ (B) and $HectD1_{1879-1966}$ (C), with the backbone displayed for all the 20 conformers and the side chains only for the lowest energy one, for the sake of clarity. (D) Superimposed backbone representation (oxygen atom of the peptide bond excluded) for $FKBP25_{1-73}$ (blue) and $HectD1_{1879-1966}$ (orange); the loops are illustrated with in a lighter shade, compared to the helices. (For interpretation of the references to colours in this figure legend, the reader is referred to the web version of this paper.)

17594, respectively. Chemical shift perturbations (CSPs) for $FKBP25_{1-73}$ were measured from HSQCs on adding unlabeled $YY1_{293-350}$ to 300 μM $FKBP25_{1-73}$ up to three-fold excess of YY1, in 10 mM Tris 300 mM NaCl, 10 mM DTT and 187 μM $ZnCl_2$ (higher amounts led to precipitation). Background minor CSPs from $ZnCl_2$ addition to FKBP25 alone were corrected for. In the absence of Zn^{2+}, no CSPs were observed.

2.3. Bioinformatic evaluation

ConSurf was used to structurally analyze conserved regions of $FKBP25_{1-73}$ and $HectD1_{1879-1966}$. ConSurf uses a multiple sequence alignment to map the level of conservation upon the protein structure [24,25]. The multiple sequence alignment was created by MUSCLE v3.8 using sequence homologs to $FKBP25_{1-73}$ and

HectD1$_{1879–1966}$. The homologs were identified by running the sequences of FKBP25 (Refseq, NP_002004.1) and HectD1 (GenBank, BAG54248.1) in Blastp against the protein sequence database NR, choosing one representative sequence for each species.

3. Results and discussion

The structure of the N-terminal domain of FKBP25$_{1–73}$, comprising the 8.4 kDa N-terminal domain of the full-length protein, as presented here (Fig. 1) was determined by high-resolution NMR spectroscopy. Coordinates of FKBP25$_{1–73}$ were deposited in the PDB as 2KFV and its resonance assignment in the BioMagResBank (BMRB) as entry 16189. The statistics for the NMR structure, comprising an ensemble of the 20 lowest energy conformers, are reported in Table 1. The N-terminal domain of FKBP25 was originally predicted as a Helix-Loop-Helix motif, characteristic of transcription factors and DNA-binding proteins [26], with the two helices corresponding to residues 7–19 and 33–50 and linked by a loop [7]. Here we show that this prediction was incorrect. Our FKBP25$_{1–73}$ structure (Fig. 2A) shows an entirely different fold where the two predicted helical regions present five structurally distinct but well-bundled helices (H1: 11–17; H2: 22–33; H3: 34–41; H4: 46–52; H5: 55–70). All secondary structure elements wrap around a common hydrophobic core, composed predominantly of the aliphatic amino acids alanine and leucine, which are abundant in a high number in the sequence (11% for alanine and 11% for leucine). Four alanines at the disordered N-terminus end do not participate in the core. At 12.3%, lysine is another abundant amino acid that confers a basic nature to the domain; the pI of the domain is 9.63. Interestingly, 6 out of 9 lysines (K22, K23, K27, K48, K52 and K56) are closely localized on the structure, thereby creating a continuous positive patch. This surface area comprises H2, the N-terminal end of H5, and H4 (Fig. 2B). Analysis of the conservation of the protein sequence is mapped onto the structure showed one significant continuous conserved surface patch, including residues K22, K23, N49, K52, T53 and K56 (Fig. 2C), which are highly conserved over a wide range of species ranging from sea anemones to human. The spatial overlap of this conserved surface region with the positive surface patch indicates an evolutionary conserved functional role. The positive charge of this motif and its protruding shape may represent a major groove – binding motif and could represent the structural basis of how the N-terminal domain of FKBP25 binds DNA [7].

Table 1
Structural statistics of the 20 best-fit NMR structures of FKBP25$_{1–73}$ (2KFV) and HectD1$_{1879–1966}$ (2LC3).

	2KFV[a]	2LC3[a]
A. NMR restraints		
Distance restraints		
Total NOE	1527	2366
Intra residue (|i−j| = 0)	740	500
Sequential (|i−j| = 1)	435	611
Medium range (2 ⩽ |i−j| ⩽ 4)	401	632
Long range (|i−j| > 4)	386	623
Hydrogen bonds	28	0
Dihedral angle restraints		
φ	49	76
ψ	49	76
RDC restraints		
$^1D_{NH}$	37	0
$^1D_{NC'}$	51	0
$^1D_{C'C\alpha}$	50	0
B. Structure ensemble statistics		
Violations		
Distance constraints (>0.5 Å)	0	0
Dihedral angle constraints (>10°)	0	0.25 ± 0.43
Deviations from ideal geometry		
Bond lengths (Å)	0.0133 ± 0.0002	0.0135 ± 0.0002
Bond angles (°)	0.899 ± 0.0166	0.891 ± 0.018
Impropers (°)	1.81 ± 0.11	1.84 ± 0.11
Ramachandran plot[b]		
Residues in most favored regions (%)	94.2	89.4
Residues in additionally allowed regions (%)	5.8	10.6
Residues in generously allowed regions (%)	0	0
Residues in disallowed regions (%)	0	0
Average pairwis e r.m.s.d.[c] *(Å)*		
Backbone	0.67 ± 0.13	0.47 ± 0.09
Heavy	1.42 ± 0.23	0.96 ± 0.12
Global quality score (Z-score)		
Verify3D	−1.12	−0.80
ProsaII	0.54	1.20
Procheck (phi–psi)	1.02	0.12
Procheck (all)	−0.06	−1.06
MolprobityClashscore	−0.67	−0.81

[a] Ensemble of 20 lowest-energy structures out of 100 calculated.
[b] Values calculated for the ordered regions, as reported by PSVS[11]: 2LC3, residues 2–7, 9–82; 2FKV, residues 27–91.
[c] 2LC3, residues 15–79; 2FKV, residues 27–91.

To molecularly map the interaction between FKBP25$_{1–73}$ and YY1 [9], CSPs on ^{15}N-labelled FKBP25$_{1–73}$were measured in HSQC titrations with unlabeled YY1$_{293–350}$, comprising the proposed FKBP25 interaction site YY1$_{300–333}$ [9]. Only FKBP25$_{1–73}$ residues A3, E31, H32, L38 and K73 were found to show significant YY1$_{293–350}$-dependent CSPs in the presence of Zn^{2+}, ranging from 0.05 to 0.12 ppm; notably, these residues are clustered, but the location of this cluster is distant from the positively charged surface described above (Fig. 2C). Only residue L38 in this patch is conserved between FKBP25$_{1–73}$ and HectD1$_{1879–1966}$, suggesting that the YY1 binding site is not preserved in HectD1. However, since the interaction surface of YY1 and the positive, possibly DNA-binding, surface do not overlap structurally (Fig. 2C), the enhanced DNA binding activity of YY1 on binding FKBP25 [9] could be due to allosteric effects and/or YY1 recruitment of an additional DNA-binding motif in FKBP25.

The only other protein sequence with significant sequence similarity (∼36% identity) to FKBP25$_{1–73}$ as identified by a wide BLAST search comprised a subdomain of HectD1, including residues 1879–1966 in human. To find out if this domain had the same fold as FKBP25$_{1–73}$, we determined the structure of HectD1$_{1879–1966}$ by NMR. The structure of the 10 kDa HectD1$_{1879–1966}$ was deposited in the PDB as 2LC3 and in the BMRB as entry 17594. Its core domain aligns to FKBP25$_{1–73}$ with a RMSD of 0.796 Å for the backbone and 1.148 for all the atoms (2KFV: 11–70; 2LC3: 1895–1958). Statistics for the NMR structure of HectD1$_{1879–1966}$ are listed in Table 1, with the 20 lowest energy conformers shown in Fig. 1. Similar to FKBP25$_{1–73}$, HectD1$_{1879–1966}$ is composed of five core helices: an additional small helix N-terminal to the core is also present (H0: 1882–1887; H1: 1895–1903; H2: 1909–1921; H3: 1922–1929; H4: 1934–1942; H5: 1943–1958) (Fig. 2D). Although the HectD1 domain is also composed of a high percentage of lysine (12.5%, pI: 8.45), only 3 lysines out of 11 (K1910, K1936 and K1940, corresponding to K22, K48 and K52 in FKBP25$_{1–73}$ respectively) cluster, but together with residues R49, K52 and R64, from H3, H4 and the loop joining them, these residues jointly produce a wide positively-charged surface area in the same region as in FKBP25$_{1–73}$ (Fig. 2E). The role of this basic patch is unknown.

To evaluate the uniqueness of the fold we searched for further structural homologs folds using DALI [27]. Other than FKBP25 and HectD1, which had a high DALI Z-scores of 9.3, DALI found only one other hit with a *Z*-score >4: the central region of an AAA ATPase, (PDB: 2QW6) with a *Z*-score of 4.2. Upon closer inspection, we found that although the orientation of core helices H1, H2 and H5 is similar in 2QW6, the resemblance to H3 and H4 in FKBP25$_{1–73}$

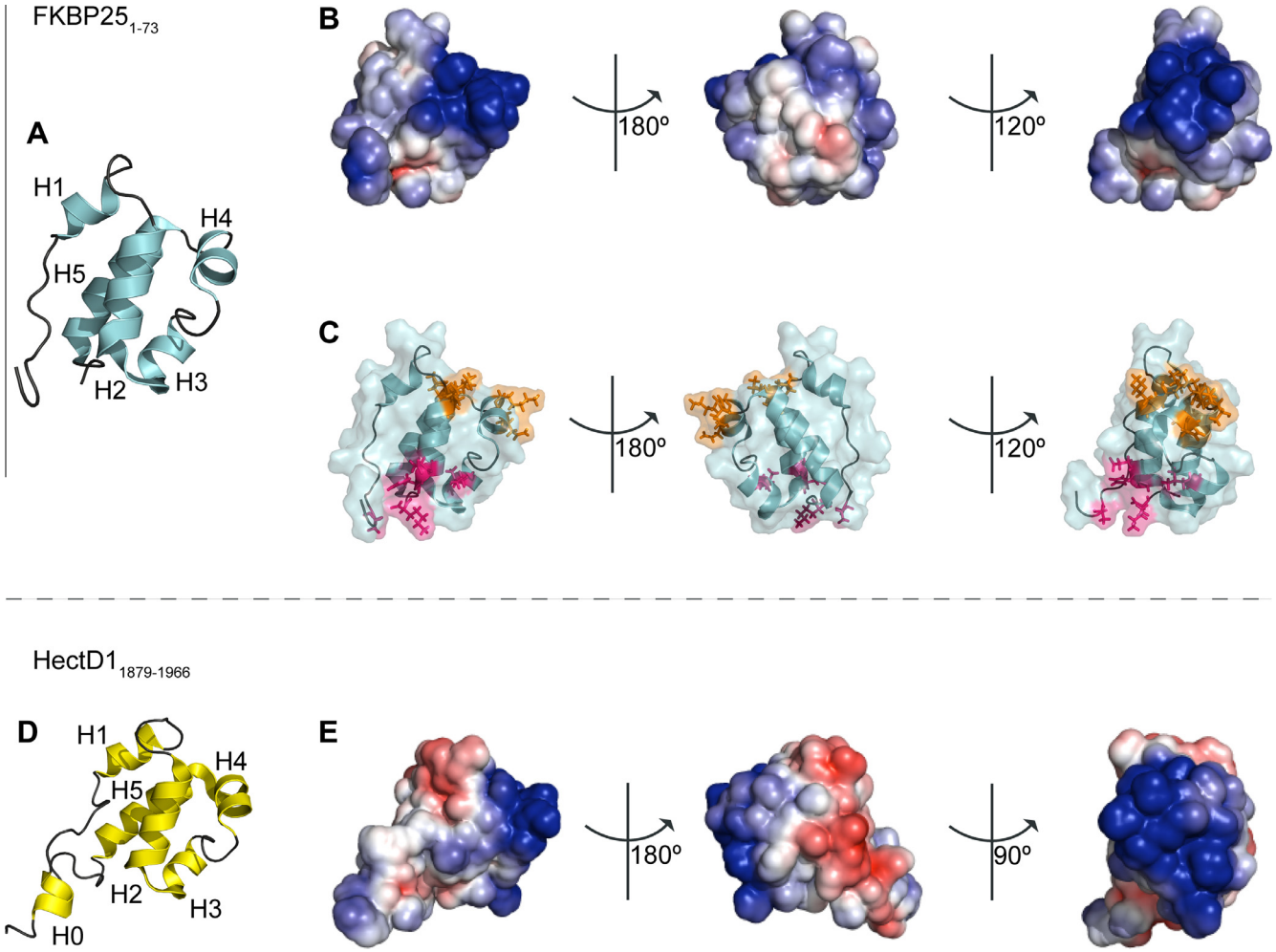

Fig. 2. Ribbon diagram (A, D) and electrostatics surface (B and E) for the structure of FKBP25$_{1-73}$ (A and B) and HectD1$_{1879-1966}$ (D and E), respectively. Surface-exposed, evolutionary conserved residues (orange) and YY1 interaction surface (magenta) are highlighted in (C) for FKBP25$_{1-73}$. The electrostatic surface representations were rotated of an appropriate angle in the last view to show in the best way for each structure the wide electrostatic patch. (For interpretation of the references to colours in this figure legend, the reader is referred to the web version of this paper.)

and HectD1$_{1879-1966}$ is poor. These two helices are short (6–8 amino acids) compared to the other helices but their most interesting characteristic is their relative position. While the three other core helices tend to assume more a parallel/bundle-like conformation, helices H3 and H4 are tilted, with H4 almost perpendicular to H5, and similar relative orientations between H3 and H4 (34° for FKBP25$_{1-73}$ and 38° for HectD1$_{1879-1966}$). It appears that while the relative positions of helices 1, 2 and 5 are similar to what is observed for classic helix bundles, helices comparable to the tilted helices H3 and H4 are found only in FKBP25$_{1-73}$ and HectD1$_{1879-1966}$. Notably, these tilted helices also present the basic patch present in both domains.

Taken together, this work describes the structure of a unique N-terminal domain motif in the FKBP family, FKBP25$_{1-73}$, and its structurally homologous domain HectD1$_{1879-1966}$. In contrast to previous predictions suggesting a HLH motif for this domain [7], our high-resolution structures show a new fold composed of five small helices where H3 and H4 are tilted in a novel arrangement; we call this fold the Basic Tilted Helix Bundle (BTHB) domain. Our structural analysis of this fold motif suggests that the DNA binding properties of FKBP25$_{1-73}$ are mediated by the conserved basic motif, which is also present in HectD1$_{1879-1966}$. Amino acids participating in FKBP25$_{1-73}$ binding of YY1 are located distant from the DNA binding site and are not conserved in HectD1$_{1879-1966}$. Structural analysis therefore suggests a fold-uniting basic binding motif, which could be allosterically fine-tuned by adjacent regulatory proteins and/or protein domains.

Acknowledgments

This work was supported in part by grants from the Natural Sciences and Engineering Research Council of Canada (CHA), the Swedish Research Council (MS), the Swedish Cancer Society (MS), the Swedish Governmental Agency for Innovation Systems VINNOVA (MS), and the National Institutes of Health through Northeast Structural Genomics Consortium (U54 GM094597). The SGC is a registered charity (number 1097737) that receives funds from AbbVie, Boehringer Ingelheim, Canada Foundation for Innovation, the Canadian Institutes for Health Research, Genome Canada through the Ontario Genomics Institute [OGI-055], GlaxoSmithKline, Janssen, Lilly Canada, the Novartis Research Foundation, the Ontario Ministry of Economic Development and Innovation, Pfizer, Takeda, and the Wellcome Trust [092809/Z/10/Z],

References

[1] C.B. Kang et al., FKBP family proteins: immunophilins with versatile biological functions, Neurosignals 16 (4) (2008) 318–325.

[2] A. Galat, Functional diversity and pharmacological profiles of the FKBPs and their complexes with small natural ligands, Cell. Mol. Life Sci. 70 (18) (2013) 3243–3275.
[3] Y.J. Jin, S.J. Burakoff, B.E. Bierer, Molecular cloning of a 25-kDa high affinity rapamycin binding protein, FKBP25, J. Biol. Chem. 267 (16) (1992) 10942–10945.
[4] Y.L. Yao et al., FKBPs in chromatin modification and cancer, Curr. Opin. Pharmacol. 11 (4) (2011) 301–307.
[5] J. Liang et al., Structure of the human 25 kDa FK506 binding protein complexed with rapamycin, J. Am. Chem. Soc. 118 (5) (1996) 1231–1232.
[6] Y.J. Jin, S.J. Burakoff, The 25-kDa FK506-binding protein is localized in the nucleus and associates with casein kinase II and nucleolin, Proc. Natl. Acad. Sci. USA 90 (16) (1993) 7769–7773.
[7] S. Riviere, A. Menez, A. Galat, On the localization of FKBP25 in T-lymphocytes, FEBS Lett. 315 (3) (1993) 247–251.
[8] M. Eitoku et al., Histone chaperones: 30 years from isolation to elucidation of the mechanisms of nucleosome assembly and disassembly, Cell. Mol. Life Sci. 65 (3) (2008) 414–444.
[9] W.M. Yang, Y.L. Yao, E. Seto, The FK506-binding protein 25 functionally associates with histone deacetylases and with transcription factor YY1, EMBO J. 20 (17) (2001) 4814–4825.
[10] A.A. Sarkar, I.E. Zohn, Hectd1 regulates intracellular localization and secretion of Hsp90 to control cellular behavior of the cranial mesenchyme, J. Cell Biol. 196 (6) (2012) 789–800.
[11] H. Tran et al., HectD1 E3 ligase modifies adenomatous polyposis coli (APC) with polyubiquitin to promote the APC-axin interaction, J. Biol. Chem. 288 (6) (2013) 3753–3767.
[12] H.B. Houbaviy et al., Cocrystal structure of YY1 bound to the adeno-associated virus P5 initiator, Proc. Natl. Acad. Sci. USA 93 (24) (1996) 13577–13582.
[13] A. Lemak et al., A novel strategy for NMR resonance assignment and protein structure determination, J. Biomol. NMR 49 (1) (2011) 27–38.
[14] Goddard, T.G., Kneller, D.G., 2007. SPARKY 3, University of California, San Francisco.
[15] P. Guntert, Automated NMR structure calculation with CYANA, Methods Mol. Biol. 278 (2004) 353–378.
[16] M. Ottiger, F. Delaglio, A. Bax, Measurement of J and dipolar couplings from simplified two-dimensional NMR spectra, J. Magn. Reson. 131 (2) (1998) 373–378.
[17] P. Permi, A. Annila, Transverse relaxation optimised spin-state selective NMR experiments for measurement of residual dipolar couplings, J. Biomol. NMR 16 (3) (2000) 221–227.
[18] P. Schanda, H. Van Melckebeke, B. Brutscher, Speeding up three-dimensional protein NMR experiments to a few minutes, J. Am. Chem. Soc. 128 (28) (2006) 9042–9043.
[19] V.Y. Orekhov, I. Ibraghimov, M. Billeter, Optimizing resolution in multidimensional NMR by three-way decomposition, J. Biomol. NMR 27 (2) (2003) 165–173.
[20] M. Zweckstetter, G. Hummer, A. Bax, Prediction of charge-induced molecular alignment of biomolecules dissolved in dilute liquid-crystalline phases, Biophys. J. 86 (6) (2004) 3444–3460.
[21] A.T. Brunger et al., Crystallography & NMR system: a new software suite for macromolecular structure determination, Acta Crystallogr. D Biol. Crystallogr. 54 (Pt 5) (1998) 905–921.
[22] J.P. Linge et al., ARIA: automated NOE assignment and NMR structure calculation, Bioinformatics 19 (2) (2003) 315–316.
[23] A. Bhattacharya, R. Tejero, G.T. Montelione, Evaluating protein structures determined by structural genomics consortia, Proteins 66 (4) (2007) 778–795.
[24] G. Celniker et al., ConSurf: using evolutionary data to raise testable hypotheses about protein function, Isr. J. Chem. 53 (3–4) (2013) 199–206.
[25] H. Ashkenazy et al., ConSurf 2010: calculating evolutionary conservation in sequence and structure of proteins and nucleic acids, Nucleic Acids Res. 38 (2010) W529–W533.
[26] M.E. Massari, C. Murre, Helix-loop-helix proteins: regulators of transcription in eucaryotic organisms, Mol. Cell. Biol. 20 (2) (2000) 429–440.
[27] L. Holm, J. Park, DaliLite workbench for protein structure comparison, Bioinformatics 16 (6) (2000) 566–567.